EPS: An Efficient Electrochemical-Polarization System Model for Real-Time Battery Energy Storage Systems in Autonomous EVs

Qasim Ajao, Olukotun Oludamilare, and Lanre Sadeeq (IEEE Members)

***Abstract*—This article introduces a new Electrochemical-Polarization System (EPS) Model to improve lithium-ion battery models for autonomous electric vehicles (AEVs). The model incorporates an additional RC network to capture the relaxation effect in these batteries. The Nernst model is used to express the open-circuit voltage as a function of State of Charge (SoC), eliminating the need for time-consuming tests. Model parameters are estimated using the least squares method with data from a hybrid power pulse characteristic test. Experimental results validate the accurate simulation of battery behavior over time. Implementing this model and parameter determination approach eliminates the need for laborious tests traditionally used for parameter calibration.**

Impact Statement: The demand for better lithium-ion battery models in autonomous electric vehicles (AEVs) requires improvements to make them more suitable. Current modeling approaches for these batteries face challenges in accurately capturing their dynamic behavior, such as representing complex electrochemical processes, accounting for non-linearities and thermal effects, and incorporating aging and degradation mechanisms. Our research addresses these challenges by introducing the Electrochemical-Polarization System (EPS) Model, which integrates an additional RC network to capture the relaxation effect observed in lithium-ion batteries. We use the Nernst model to express the open-circuit voltage as a function of State of Charge (SoC), eliminating the need for time-consuming and error-prone tests. Instead, we estimate model parameters using the least squares method with data from a hybrid power pulse characteristic test. Experimental results validate the accuracy of our proposed model in simulating battery behavior over time. Implementing this model streamlines the process of achieving reliable battery modeling in AEVs by eliminating the need for laborious tests.

***Index Terms*—autonomous EVs, lithium-ion batteries, battery management systems (BMS), RC network, SOC, electrochemical-polarization**

I. INTRODUCTION

AEVs heavily depend on the performance of their battery systems. This is why lithium-ion batteries are the preferred choice for these vehicles, given their advantageous features such as high energy density, rapid charging and discharging rates, and enhanced safety [1]. Consequently, improving the accuracy of power battery models, particularly for lithium-ion batteries, has become a crucial research objective. This motivation stems from the growing interest in the dynamic simulation of AEVs, energy distribution, power control strategies, and the estimation of battery parameters such as the State of Charge SoC and the State of Health SoH [2, 3]. Given the nonlinearity of battery systems, two primary types of models have emerged: electrochemical models, which provide comprehensive descriptions of battery characteristics based on electrochemical theory and mathematical representations of internal actions [4, 5, 6]. However, accurately reproducing their dynamic behavior remains challenging [7]. To address this challenge, equivalent circuit models (ECMs) have been proposed, consisting of resistors, capacitors, and voltage sources that capture the battery's dynamic properties and operating principles [8, 9].

In ECMs, the Open Circuit Voltage (OCV) is typically determined experimentally or through calculations at specific SoC values. Nevertheless, calculating the OCV as a function of SoC within ECMs can be a time-consuming and error-prone process. Moreover, the discrete representation of OCV across multiple SoCs complicates the implementation of SoC estimation methods based on Kalman filtering and observers.

In this paper, our focus is on a $\mathrm{LiFePO_4}$ battery module with a nominal capacity of 12 Ah and an operating voltage of 32 V. $\mathrm{LiFePO_4}$ batteries are rechargeable lithium-ion (Li-Ion) batteries known for their advantages over traditional cobalt-based Li-Ion batteries, including increased power output, quicker charging, reduced weight, and prolonged lifespan. To establish an explicit relationship between OCV and SoC, without the need for dedicated OCV determination experiments under different loading profiles, we propose a novel electrochemical-polarization system (EPS) model. This model incorporates an RC network to accurately represent the battery's dynamic relaxation effect. The model parameters are determined using the least-squares (LS) approach. Additionally, the correctness of the model is verified through dynamic stress testing (DST).

II. LITERATURE REVIEW

Modeling lithium-ion batteries used in autonomous electric vehicles (AEVs) follows a similar approach to the modeling process employed for electric vehicles. However, AEVs introduce additional considerations regarding vehicle autonomy and computational requirements [10]. Fundamental electrochemical modeling processes within lithium-ion batteries remain

consistent for AEVs. However, the modeling should account for distinct usage patterns, such as frequent acceleration and deceleration, which may impact battery performance and aging [11]. Additionally, the modeling should address dynamic loads imposed by the computational systems used for autonomous driving, as these systems require substantial power and can influence battery behavior [12].

Thermal management assumes heightened importance in AEVs due to the computational workload involved in autonomous driving. The battery pack must effectively manage the increased heat generated not only during charging and discharging but also by the computational components. Advanced Thermal modeling techniques are employed to accurately predict and regulate temperature distribution within the battery pack, ensuring optimal performance, safety, and longevity [13].

Analogous to electric vehicles, mechanical modeling for Autonomous EVs primarily revolves around analyzing the battery pack's structural integrity to withstand mechanical stresses during vehicle operation. Nevertheless, AEVs may necessitate additional modeling considerations to account for the weight and placement of computational hardware, as well as any vibrations or impacts that could affect the battery's mechanical stability [14]. AEVs frequently operate in challenging environments involving frequent start-stop scenarios and rapid acceleration and deceleration. These conditions can expedite battery aging and degradation. Modeling must incorporate the impact of increased usage and demanding driving conditions on battery lifespan, state of health, and degradation mechanisms. By comprehending and mitigating these factors, optimal battery design and management strategies can be developed to extend battery life [15].

Typically, AEVs rely on intricate control and management systems to enable autonomous driving [14]. Modeling these systems is pivotal for optimizing battery operation and ensuring efficient energy management. Additionally, the modeling may incorporate algorithms and predictive models to estimate future energy demands based on the driving route, traffic conditions, and computational requirements of autonomous systems. This ensures that battery performance aligns with the demands of autonomous driving while upholding safety and reliability. Modeling for lithium-ion batteries used in AEVs builds upon existing methodologies employed for electric vehicles while considering supplementary factors associated with computational requirements and vehicle autonomy [16]. By incorporating these considerations into the modeling process, researchers and engineers can optimize battery design, enhance efficiency, prolong the lifespan, and elevate the overall performance and safety of AEVs.

III. LITHIUM-ION BATTERY MODELS

Various types of batteries exist, and their performance is influenced by different factors. Mathematical models have been developed to predict battery performance, and they are widely used in electric vehicle (EV) research. One such model is the Equivalent Circuit Model (ECM), which includes

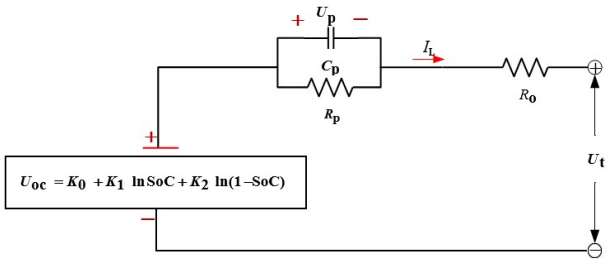

Fig. 1. Schematic for The Novel EPS Model.

sub-models such as Rint, RC, Thevenin, PNGV, and others. Additionally, other models like the Nernst model, combination model, Unnewehr universal model, and Shepherd model are commonly employed as well. In this paper, we propose a novel model called the Electrochemical-Polarization System (EPS) model for autonomous electric vehicles (AEVs). This model enhances the polarization characteristics of the Nernst model and captures the internal behavior of the Thevenin model specifically for lithium-ion batteries. The EPS model is utilized to achieve these improvements.

Figure 1 depicts the schematic diagram of the developed EPS variant model. The Nernst model is utilized to model the Open Circuit Voltage (OCV), represented as U_{oc}, in relation to the State of Charge (SoC).

$$\begin{cases} U_{\mathrm{t}} = U_{\mathrm{oc}} - U_{\mathrm{p}} - I_{\mathrm{L}} R_{\mathrm{o}} \\ \dot{U}_{\mathrm{p}} = \frac{I_{\mathrm{L}}}{C_{\mathrm{p}}} - \frac{U_{\mathrm{p}}}{C_{\mathrm{p}} R_{\mathrm{p}}} \\ U_{\mathrm{oc}} = K_0 + K_1 \ln SoC + K_2 \ln(1 - SoC) \end{cases} \tag{1}$$

The model incorporates three carefully selected constants (K_0, K_1 and K_2) to ensure accurate fitting of the data. R_{o} represents ohmic resistance, R_{p} represents polarization resistance, and C_{p} represents the transient response during charging, and discharging in the EPS model. The voltage measured across C_{p} is denoted as U_{p}.

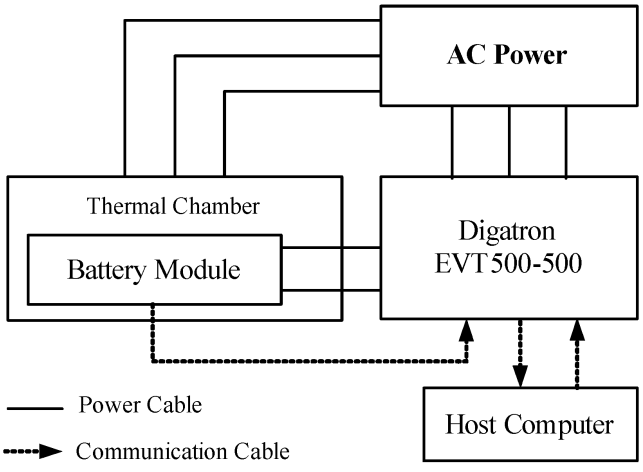

Fig. 2. The Developed Battery Test Bench

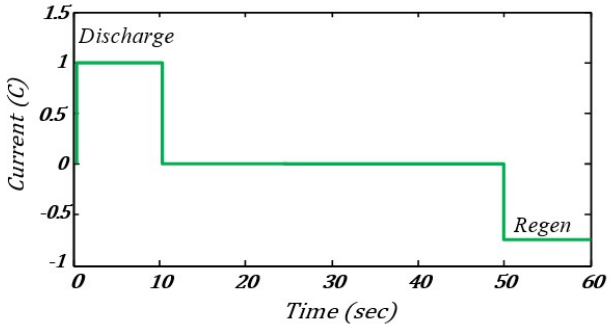

Fig. 3. The Current Profile for HPPC

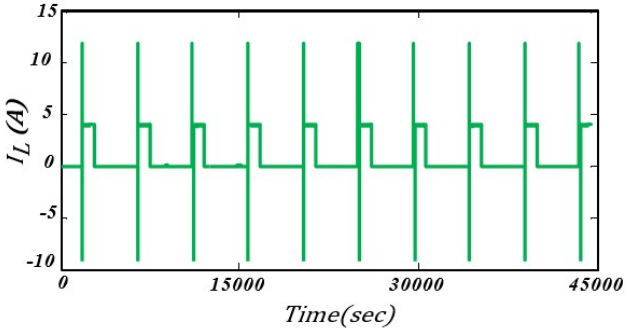

Fig. 4. The Current Profiles for HPPC Test

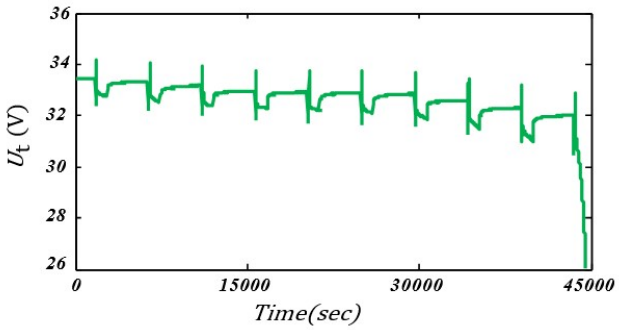

Fig. 5. The Voltage Profiles for HPPC Test

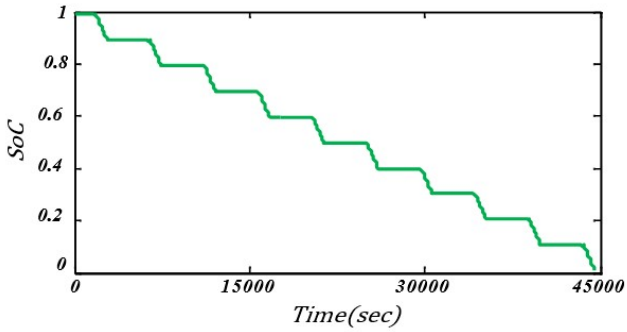

Fig. 6. The SoC Calculated Profiles for HPPC Test

Equation (1) presented below accurately describes the electrical behavior of the model. The battery test bench, as depicted in Figure 2, was specifically designed to suit the configuration of the AEV for this study. The central component, Digatron EVT500-500, has the capacity to charge and discharge battery modules. It has voltage and current limits set at 500 V and 500 A, respectively, representing their maximum values.

Additionally, it allows for rapid measurement of critical parameters, including voltage, current, and temperature. The host computer, equipped with BTS-600 software, enables the creation of experimental protocols and facilitates real-time data acquisition. To minimize the influence of temperature on model parameters, all evaluations involving the $\mathrm{LiMn2O_4}$ battery module are conducted within a thermal chamber maintained at a constant temperature of 20°C.

IV. MODELING AND PARAMETERIZATION

A. The Identification of Model Parameters

In order to determine the model parameters, a battery test bench is developed with the purpose of facilitating the estimation of both the model structure and the unknown parameters (refer to Figure 2). The recognition process aims to make estimations based on specific criteria and utilize measurement information obtained from known systems as a reference. By conducting meticulous analysis and comparison of the collected data, the test bench aims to achieve accurate estimations for the model's structure and the values of the unknown parameters. This effort contributes to a comprehensive understanding of the battery system, thereby refining the accuracy and effectiveness of the model in predicting and analyzing its behavior.

1) Design and Experiments: The experimental setup used in this paper is depicted in Figure 2. To gather the required data for parameter identification, a Hybrid Pulse Power Characterization (HPPC) test method, as described in [10], is conducted on the $\mathrm{LiFePO_4}$ battery module. The discharge segments of this test are performed at a constant current of C/3, with intervals of 0.1 State of Charge (SoC) ranging from 1.0 to 0.1. After each interval, a two-hour break is introduced to allow the battery to reach a state of electrochemical and thermal equilibrium before proceeding to the next interval.

Figure 2 shows the HPPC current profile, while Figures 3, 4, 5, and 6 illustrate the current, voltage, and calculated SoC profiles of the HPPC test, respectively. It is important to note that all figures are presented on the same scale to facilitate comparison. The measurements are sampled at a frequency of one second to ensure accurate data acquisition.

2) Method for the Parameters Identification: Discretization is a widely used technique in numerical methods and simulations as it enables the approximation of continuous systems and equations using discrete computational approaches, thereby facilitating their solvability. This mathematical procedure involves replacing the continuous variables and derivatives in the original equation with their discrete counterparts, allowing the equation to be expressed in terms of discrete

values or intervals. The discrete form of Equation (1) can be derived by using the first-order backward difference and substituting U_{oc} with $K_0 + K_1 \ln SoC + K_2 \ln(1 - SoC)$:

$$\begin{aligned} U_{\mathrm{t}}(k) = c_1 + c_2 U_{\mathrm{t}}(k-1) + c_3 \ln(SoC(k)) + c_4 \\ \ln(1 - SoC(k)) + c_5 I_{\mathrm{L}}(k) + c_6 I_{\mathrm{L}}(k-1) \end{aligned} \tag{2}$$

Where:

$$\begin{aligned} c_1 = \frac{TK_0}{T + R_{\mathrm{p}}C_{\mathrm{p}}}, c_2 = \frac{R_{\mathrm{p}}C_{\mathrm{p}}}{T + R_{\mathrm{p}}C_{\mathrm{p}}}, \\ c_3 = \frac{TK_1}{T + R_{\mathrm{p}}C_{\mathrm{p}}}, c_4 = \frac{TK_2}{T + R_{\mathrm{p}}C_{\mathrm{p}}}, \\ c_5 = -\frac{TR_{\mathrm{o}} + TR_{\mathrm{p}} + C_{\mathrm{p}}R_{\mathrm{p}}R_{\mathrm{o}}}{T + R_{\mathrm{p}}C_{\mathrm{p}}}, c_6 = \frac{C_{\mathrm{p}}R_{\mathrm{p}}R_{\mathrm{o}}}{T + R_{\mathrm{p}}C_{\mathrm{p}}} \end{aligned} \tag{3}$$

In the context of parameter identification, the computation of model parameters can be achieved using the following formula, assuming that the sample intervals T are uniformly set to one second:

$$\begin{aligned} K_0 = \frac{c_1}{1 - c_2}, K_1 = \frac{c_3}{1 - c_2}, K_2 = \frac{c_4}{1 - c_2}, \\ R_{\mathrm{o}} = \frac{c_6}{c_2}, R_{\mathrm{p}} = \frac{c_2 c_5 + c_6}{c_2^2 - c_2}, C_{\mathrm{p}} = \frac{T_{\mathrm{s}} c_2^2}{c_2 - c_2^2} \end{aligned} \tag{4}$$

This approach enables the estimation of model parameters for the given system. The parameters can be obtained in a closed form by utilizing the principles of least-squares estimation. This involves analyzing a set of N cell input-output three-tuples, denoted as $\{y(k) \quad I_{\mathrm{L}}(k) and \quad SoC(k)\}$:

$$\mathbf{Y} = \begin{bmatrix} y(1) & y(2) & \cdots & y(N) \end{bmatrix}^{\mathrm{T}} \tag{5}$$

And the matrix:

$$\mathbf{H} = \begin{bmatrix} \varphi(1) & \varphi(2) & \cdots & \varphi(N) \end{bmatrix}^{\mathrm{T}} \tag{6}$$

$$\varphi(k) = \begin{bmatrix} 1 & U_{\mathrm{t}}(k-1) & \ln(SoC(k)) & \\ & \ln(1 - SoC(k)) & I_{\mathrm{L}}(k) & I_{\mathrm{L}}(k-1) \end{bmatrix}^{\mathrm{T}} \tag{7}$$

In this paper, an off-line (batch) approach is employed to solve for these parameters. The subsequent steps outline the sequential process for constructing the vector in the correct order. In the following analysis, we consider the relationship between $\mathbf{Y} = \mathbf{H}\boldsymbol{\theta}$, where $\boldsymbol{\theta} = \begin{bmatrix} c_1 & c_2 & c_3 & c_4 & c_5 & c_6 \end{bmatrix}^{\mathrm{T}}$ is associated with the vector of unknown parameters. Drawing upon the result from least-squares estimation theory, we solve for the parameters $\boldsymbol{\theta}$ using the known matrices $\mathbf{Y}$. and $\mathbf{H}$. and employing an approach based on least-squares estimation. This methodology enables us to obtain accurate parameter estimates for $\boldsymbol{\theta} = \left(\mathbf{H}^{\mathrm{T}}\mathbf{H}\right)^{-1}\mathbf{H}^{\mathrm{T}}\mathbf{Y}$.

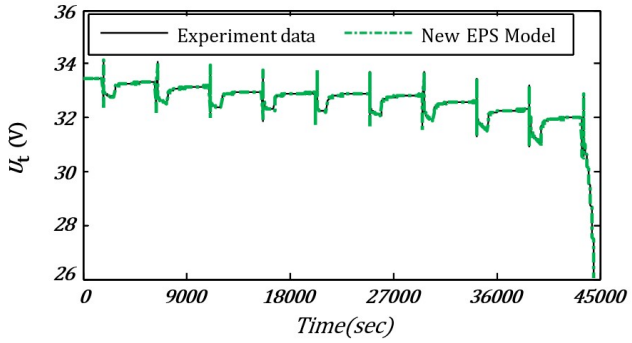

Fig. 7. Terminal Voltage Profiles of the New EPS Model

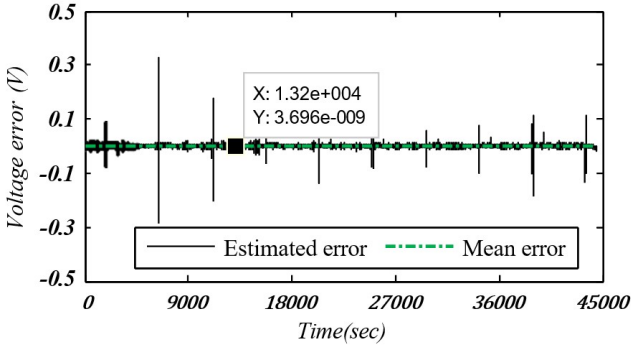

Fig. 8. Estimated Values and Experiment Data Error Profiles

V. RESULTS

The identification result is displayed in Table 1. The terminal voltage comparison curves, which illustrate the experimental data and model-based estimated values, are presented in Figures 7 and 8.

Table 1. Results Identification for the New EPS Model

K_0	K_1	K_2	$R_{\mathrm{p}}(\Omega)$	$C_{\mathrm{p}}(\mathrm{F})$	$R_{\mathrm{o}}(\Omega)$
35.644	1.9064	0.5270	0.3801	124.255	0.0828

These curves are specifically shown in Figure 7, and the findings depicted in these figures effectively demonstrate the accuracy of the newly proposed EPS model in assessing the terminal voltage. The maximum error observed as shown in Figure 8 is below 0.5V, taking into account the nominal voltage of 32V.

A. Results Verification

The evaluation of battery models and State of Charge (SoC) estimation algorithms often relies on the Dynamic Stress Test (DST), which involves a 360-second sequence comprising seven distinct power levels applied in a step-wise manner [11].

Table 2. Results Identification for the New EPS Model

K_0	K_1	K_2	$R_{\mathrm{p}}(\Omega)$	$C_{\mathrm{p}}(\mathrm{F})$	$R_{\mathrm{o}}(\Omega)$
32.009	0.4299	0.0347	0.3121	169.261	0.0765

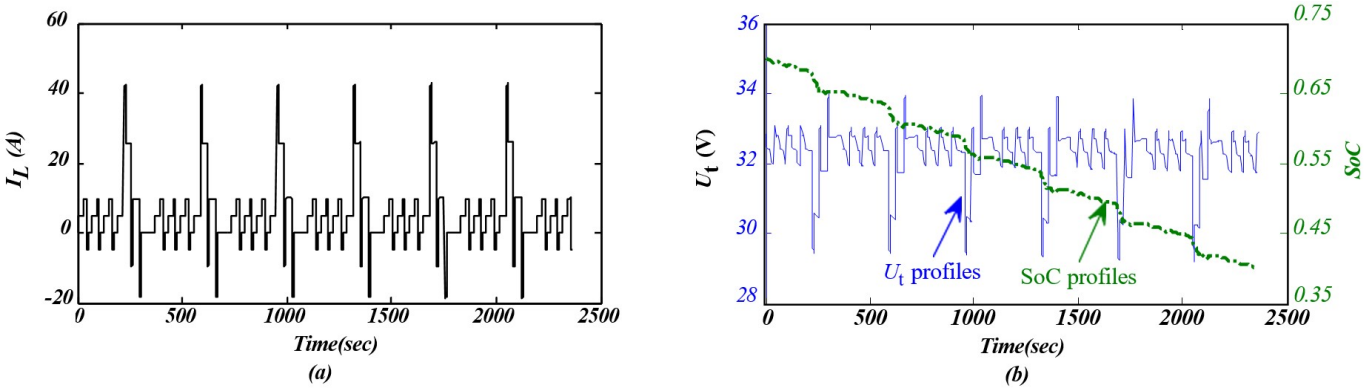

Fig. 9. (a) Current Profiles in the DST (b) SoC and the Voltage Profiles in the HDST test, with SoC values ranging from 0.4 to 0.7.

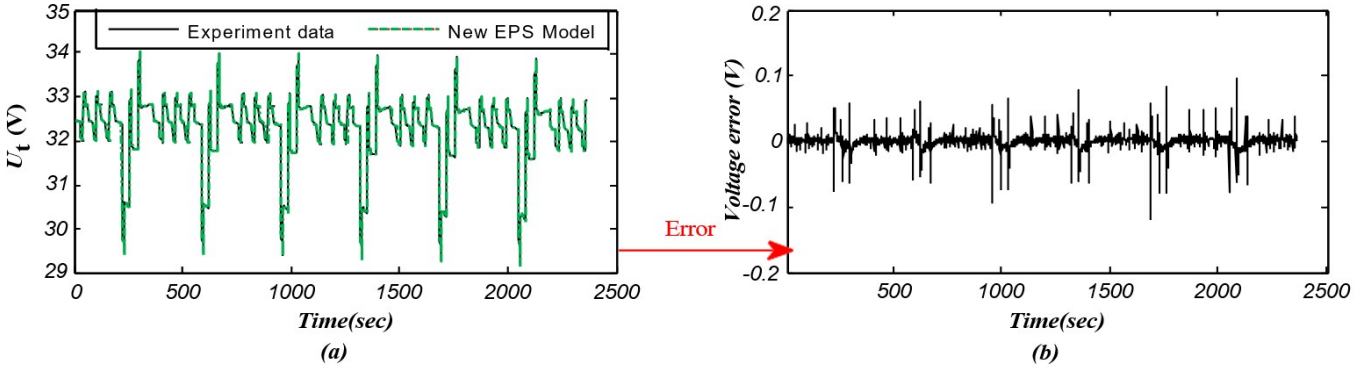

Fig. 10. (a) The Voltage Curves of the Experimental Data and (b) the Model-Based Simulation Data Compared.

As a widely used standard driving cycle, the DST was employed in this study to assess the performance of the proposed battery model. A total of six consecutive DST cycles were conducted to evaluate its effectiveness. The sampled current profiles are presented in Figure 9(a), while Figure 9(b) displays the corresponding terminal voltage profiles and SoC profiles, providing a comprehensive representation of the results. Based on the methodological framework proposed for parameter identification, the specific model parameters have been determined and are presented in detail in Table 2. Figure 10 showcases a side-by-side analysis of the terminal voltage profiles obtained from the experimental measurements and the model-based simulation results. The model parameters used in the simulation were derived from the data obtained through Dynamic System Testing (DST). This comparison was carried out utilizing the model parameters extracted from the DST data as shown in Figure 10. The results indicate that the constructed EPS model exhibits exceptional dynamic performance, displaying a maximum error rate below 1%.

VI. FUTURE WORK

A. Kalman Filter Analysis and Application to AEVs

The Kalman filter is a commonly utilized state estimator that predicts the future state of a system. However, it is limited to linear systems, while many real-world scenarios, such as battery state estimates, involve nonlinear systems. To address this constraint, the extended Kalman filter (EKF) was developed specifically for nonlinear systems. Nonetheless, there are limitations on the precision of the EKF. The sigma point Kalman filter (SPKF) is proposed as an alternative method to overcome these precision issues. Among the subsets of the SPKF, the unscented Kalman filters (UKFs) and center difference Kalman filters (CDFKs) are notable examples. This research focuses on comparing and contrasting these algorithms, including their square root variants, for real-time onboard Battery Management Systems (BMS). The aim is to determine the most suitable algorithm in terms of accuracy and computing complexity.

1) Extended Kalman Filter: The extended Kalman filter (EKF) is the nonlinear version of the linear Kalman filter. In the EKF, the current mean and covariance estimates are linearized, using differentiable functions to represent the state transition and observation models.

$$\begin{aligned} x_k &= f\left(x_{k-1}, u_k\right) + w_k \\ z_k &= h\left(x_k\right) + v_k \end{aligned} \tag{8}$$

In the given equations, the function f calculates the expected state values, while the function h calculates the predicted values. These functions are denoted by their variable names. However, since these functions cannot be directly applied to

the covariance, partial derivatives are computed instead. In the Kalman filter equations, the derivatives are calculated at each stage based on the most recent predicted values, allowing linearization of the nonlinear function around the latest estimate. It's important to note that, although the extended Kalman filter (EKF) shares similarities with the Kalman filter (KF), it often doesn't perform as well as an ideal estimator. This is particularly true when both the measurement and state transition are not linear. Additionally, if the modeling process lacks sufficient precision, the initial state estimate can be inaccurate. Moreover, the EKF frequently provides an incorrect estimate of the true covariance matrix, which introduces potential inconsistencies [17].

2) Unscented Kalman Filter (UKF): To address the limitations of the EKF, an evaluation of the UKF will be conducted. The UKF presents an alternative approach for handling the state transition of non-linear systems. This methodology incorporates the unscented transformation (UT) sampling technique, which selects sigma points around the mean. Building upon the UT method, the UKF generates sigma points and utilizes them in the calculation of resultant sigma points by passing them through a specific function. Furthermore, the mean and covariance are computed by assigning appropriate weights to the sigma points. The process of calculating these sigma points and weights follows the methodology described in the reference [16, 17].

$$\begin{aligned} \sum_k w_k &= 1 \\ \text{mean } &= x = \sum_k w_k x_k \\ \text{covariance } &= P = \sum_k w_k \left(x_k - x\right)\left(x_k - x\right)^T \end{aligned} \tag{9}$$

The overall procedure of the UKF algorithm can be summarized as follows [15]: First, select a small value for $alpha$, which determines the spread of the sigma point distribution. Next, choose a value of $beta \geq 0$ to incorporate prior knowledge of the distribution. Also, select a value of $k \geq 0$. Then, compute $2N + 1$ sigma points using the equation $lambda = \alpha(2(N + K)) - N$. These sigma points are propagated through the nonlinear transformation function $y_k = f(x_k)$, where k ranges from 0 to $2N$. Finally, calculate the weighted average $bary$ and covariance P_y using $w_k(m)$ and $w_k(c)$ as the respective weights.

The future work aims to enhance the efficiency of Lithium-ion batteries in autonomous electric vehicles (AEVs) by investigating the application of the Extended Kalman Filter (EKF) and Unscented Kalman Filter (UKF) techniques for accurate estimation of the State of Charge (SOC) of the batteries. The study involves two distinct battery models: a standard model and a modified model. To validate the performance of these models, a comparative analysis will be conducted using multiple versions of Kalman filters. The results are expected to demonstrate the superior state and output quality of model 2 compared to model 1. However, it is important to note that joint estimation, despite its potential for enhancing estimation outcomes, does not guarantee parameter accuracy due to the absence of a physical model in this specific scenario.

Furthermore, the evaluation of filters includes an assessment of their Mean Squared Error (MSE) and computational complexity time. It is worth noting that the Central Difference Kalman Filter (CDKF), in combination with the square root version, exhibits superior performance compared to other Kalman filter versions. This superiority is attributed to the CDKF's reduced computational complexity while maintaining accuracy comparable to that of the UKF and square root versions. Based on the aforementioned discussion, the CDKF is identified as the preferred choice among the various Kalman filter versions for enhancing battery estimation accuracy in AEVs [17, 18].

VII. CONCLUSION

A novel electrochemical polarization system (EPS) model is introduced to analyze real-time battery storage systems in Autonomous Electric Vehicles (AEVs). This model enhances the Nernst model by incorporating an additional RC circuit, enabling the accurate simulation of electrochemical characteristics and polarization effects. Experimental and simulation results demonstrate that the proposed EPS model exhibits exceptional dynamic performance and provides a more precise estimation of the terminal voltage. The model structure includes a parallel RC network to account for battery relaxation, offering a simple yet effective representation. By employing an offline parameters identification approach based on previously saved data, the time-consuming and complex periodic calibration experiments necessary for model error correction can be avoided. In future research, the focus will shift towards exploring Extended Kalman filtering (EKF) or other model and observer-based state of charge (SoC) estimation approaches, aimed at further enhancing the accuracy and reliability of AEV battery systems.

AUTHORS DECLARATION

The authors have no conflicts to disclose.

REFERENCES

[1] B. Kennedy, D. Patterson, and S. Camilleri, "Use of lithium-ion batteries in electric vehicles," Journal of Power Sources 90, 156–162 (2000).

[2] H. He, R. Xiong, and J. Fan, "Evaluation of lithium-ion battery equivalent circuit models for state of charge estimation by an experimental approach," energies 4, 582–598 (2011).

[3] S. Lee, J. Kim, J. Lee, and B. H. Cho, "State-of-charge and capacity estimation of lithium-ion battery using a new open-circuit voltage versus state-of-charge," Journal of power sources 185, 1367–1373 (2008).

[4] G. Plett, "Lipb dynamic cell models for kalman-filter soc estimation," in The 19th international battery, hybrid and fuel electric vehicle symposium and exhibition (2002) pp. 1–12.

[5] Q. M. Ajao, "A novel rapid dispatchable energy storage system model using autonomous electric vehicles to reduce grid dependency: Georgia southern university," (2019).

[6] G. L. Plett, "Extended kalman filtering for battery management systems of lipb-based hev battery packs: Part 1. background," Journal of Power sources 134, 252–261 (2004).

[7] T. Analytics, "Battery modeling for hev simulation by thermo analytics, inc,".

[8] V. Johnson, “Battery performance models in advisor,” Journal of power sources 110, 321–329 (2002).
[9] D. Karner and J. Francfort, “Hybrid and plug-in hybrid electric vehicle performance testing by the us department of energy advanced vehicle testing activity,” Journal of Power Sources 174, 69–75 (2007).
[10] J. P. Christophersen, “Battery test manual for electric vehicles, revision 3,” Tech. Rep. (Idaho National Lab.(INL), Idaho Falls, ID (United States), 2015).
[11] Q. M. Ajao, R. J. Haddad, and A. El-Shahat, “Comparative analysis of residential solar farm with energy storage between the usa and nigeria,” in 2019 SoutheastCon (IEEE, 2019) pp. 1–8.
[12] Q. Ajao and O. Oludamilare, “Safety challenges and analysis of autonomous electric vehicle development: Insights from on-road testing and accident reports,” arXiv preprint arXiv:2305.12665 (2023).
[13] Q. Lin, J. Wang, R. Xiong, W. Shen, and H. He, “Towards a smarter battery management system: A critical review on optimal charging methods of lithium-ion batteries,” Energy 183, 220–234 (2019).
[14] J. Van Mierlo, M. Berecibar, M. El Baghdadi, C. De Cauwer, M. Messagie, T. Coosemans, V. A. Jacobs, and O. Hegazy, “Beyond the state of the art of electric vehicles: A fact-based paper of the current and prospective electric vehicle technologies,” World Electric Vehicle Journal 12, 20 (2021).
[15] K. Fujii, “Extended kalman filter,” Reference Manual 14 (2013).
[16] M. I. Ribeiro, “Kalman and extended kalman filters: Concept, derivation and properties,”
[17] C.-p. Zhang, C.-n. Zhang, and S. Sharkh, “Estimation of real-time peak power capability of a traction battery pack used in an hev,” in 2010 Asia-Pacific Power and Energy Engineering Conference (IEEE, 2010) pp. 1–6.
[18] Haddad, Rami J., Adel El-Shahat, and Youakim Kalaani. ”Lead acid battery modeling for PV applications.” Journal of Electrical Engineering 15.2 (2015): 17.

BIOGRAPHY SECTION

To be provided.